

Texture and magneto-crystalline anisotropy of an oriented ferrimagnetic $\text{ErMn}_4\text{Fe}_8\text{C}$ powder sample

M. Morales¹, D. Chateigner² and D. Fruchart³

¹Lab. Physique de l'Etat Condensé, Université du Maine, Avenue O. Messiaen 72085 Le Mans cedex - France.

²Lab. Cristallographie et Sciences des Matériaux - ISMRA, 14050 Caen - France.

³Lab. Cristallographie -CNRS BP166 38042 Grenoble cedex 09 - France.

Keywords: 4f-3d intermetallics, interstitial compounds, X-ray quantitative texture analysis, magnetic anisotropy, magnetization curves.

Abstract. Powder samples of the ternary carbide $\text{ErMn}_4\text{Fe}_8\text{C}_{x-1}$ were oriented under a low magnetic field $H \sim 0.5$ T. Analysis of the crystallographic texture of the samples confirms that the compound is of easy plane type, in agreement with magnetization measurements and neutron diffraction experiments performed elsewhere. Both the latter techniques have revealed that the magnetic arrangement is rather complicated, as supported by competing contributions to magneto-crystalline anisotropy. However, assuming a reasonably simple expression for the magneto-crystalline anisotropy valid at high temperature only, the texture analysis performed at 300 K, has allowed simulation of the anisotropic magnetization curve for this planar ferrimagnetic structure. A comparison with the experimental magnetization curve reveals the onset of a first order magnetization process (FOMP) taking place under an applied field up to 1.8 T. The occurrence of this FOMP should result on the competition between different contributions to the magneto-crystalline anisotropy energy.

Introduction

A lot of efforts have been addressed in the last decade in order to optimize the macroscopic properties of magnets [1,2]. In this aim many groups did focus on the crystallization of new phases and on the development of new texturing processes [3,4,5]. Factually, both these tendencies result in the stabilization of very anisotropic magnetic properties. However, it is not still clear how the intrinsic anisotropic magnetic properties, which exist at the scale of the single-crystal, are transferred at the macroscopic scale as observed on polycrystalline-textured samples. In the literature, many works deal on the characterization of the anisotropic behavior like magnetization curves [6,7,8,9]. These works generally concentrate on the estimation of the crystallite distribution and the intrinsic magnetic properties (crystalline anisotropy constants, sample polarization...) from the magnetization curves, using differently defined orientation or misalignment parameters in easy-axis ferromagnetic compounds. We combine in this work two different formalisms coming from two independent fields of physics. The developed methodology takes into account the really measured orientation distribution of crystallites and shows the separation of the pure magnetic influence from the texture effect. This approach requires the quantitative determination of the orientation distribution function, a precise determination of the magnetic and crystal structures, and phases for which magnetic and crystalline structures are somehow linked at zero-field. We illustrate our modeling method by the simulation of anisotropic magnetization curves at $T = 300\text{K}$ of the oriented easy-plane ferrimagnetic $\text{ErMn}_4\text{Fe}_8\text{C}$

carbide (ThMn_{12} structure type) assuming a reasonably simple expression for the magneto-crystalline anisotropy [10,11,12].

Experimental

The starting intermetallic compound ErMn_4Fe_8 was elaborated by induction melting of the metal constituents, then carburated using the anthracene route [13] for the synthesis of the ferrimagnetic $\text{ErMn}_4\text{Fe}_8\text{C}$ carbide of ThMn_{12} structure type (Curie temperature $T_C = 370\text{K}$). The purity of the resulting phase was checked using X-ray and neutron powder diffraction [11]. Finely crushed and sieved powders (grain size $\approx 50 \mu\text{m}$) of the carbide were used to prepare two differently aligned samples by solidification of a resin-powder mixture under an applied magnetic field of 0.5 T. Both samples were 4 mm diameter and 5 mm long cylinders. One sample (A) was solidified with an applied field parallel to the axis of the cylinder, while the other (B), was rotated (10 rd/mn) around its axis [5], with an applied field perpendicular to it. Both samples have the same shape and then exhibit the same demagnetizing factor.

Magnetization measurements were carried out on the random powder and on the aligned samples using an automated extraction magnetometer in the 2-300K temperature range. Measurements were performed for the oriented powders with an applied magnetic field H parallel ($M_{//}$ magnetization, Sample A) and perpendicular (M_{\perp} magnetization Sample B) to the texturation field in order to determine the macroscopic Easy Magnetization Direction (EMD). The microscopic magnetic properties were determined by neutron diffraction experiments operated on the $\text{ErMn}_4\text{Fe}_8\text{C}$ random powder using the D1B diffractometer of the ILL (France) reactor [11].

The x-ray QTA was operated using a 4-circles diffractometer and a curved position sensitive detector, for the simultaneous acquisition of the needed pole figures, as detailed elsewhere [14]. Pole figures were measured by scanning the tilt angle of the goniometer, χ , between 0 and 70° . From the pole figures we refined the orientation distribution function (ODF) using the WIMV approach [15] and the ODF was used to recalculate the necessary quantities of the crystallite distributions for the simulations. The X-ray quantitative texture analysis has allowed the determination of the c-axes distribution of the oriented $\text{ErMn}_4\text{Fe}_8\text{C}$ carbides, later used in the anisotropic magnetization curve simulation as input information.

Formalism used in the simulation of the $M(H)$ curves at $T = 300\text{K}$

At room temperature, the high order anisotropic constants $K_2, K_3...$ are negligible in the ThMn_{12} structure type compound in comparison with K_1 , the first-order anisotropy constant [10]. As the Er-3d(Mn, Fe) exchange forces are strong, the collinear magnetic arrangement of $\text{ErMn}_4\text{Fe}_8\text{C}$ carbide can be considered as quasi-rigid. Consequently, the energy in an applied magnetic field H can be expressed at $T = 300\text{K}$ by [10]:

$$E(H) = K_1 \sin^2\theta - H.M_S \cos(\theta_0 - \theta) \quad (1)$$

with θ the angle that makes the c axis of the individual crystals with the magnetization direction, with θ_0 the angle between H and the c axes of the crystallites and with M_S the saturation magnetization. The value of M_S is obtained from the fit of the $M/H=f(1/H)$ curve [1]. Under equilibrium conditions ($dE/d\theta = 0$) and with an anisotropy field $H_A=2K_1/M_S$, determined from the magnetization curves as the junction point of the two magnetization curves measured for two perpendicular orientations, we obtain:

$$\frac{H}{H_A} = \frac{\sin \theta \cos \theta}{\sin(\theta_0 - \theta)}. \quad (2)$$

In a textured sample, the angular distribution of the magnetic moments, if they are linked to a specific direction or plane of the crystal structure in zero-field, can be described by the probability function $F(\vartheta, \varphi)$ of finding the \mathbf{c} axis in a direction given by the ϑ and φ angles. Here ϑ measures the deviation of the \mathbf{c} axes from the cylinder axis (polar angle of the $\{00\ell\}$ pole figures). The φ angle gives the location of the projection of \mathbf{c} in the plane perpendicular to the cylinder axis (azimuth of pole figures). For a random distribution (isotropic sample), $F(\vartheta, \varphi)$ takes a constant value, while for a textured sample it is a distribution that has to respect the crystallite ODF.

Results and discussion

Whatever the temperature, the magnetization measurements performed on the oriented $\text{ErMn}_4\text{Fe}_8\text{C}$ samples show that the macroscopic EMD corresponds to the measurements M_{\perp} operated on Sample B (e.g. at $T = 300\text{K}$, Figure 1).

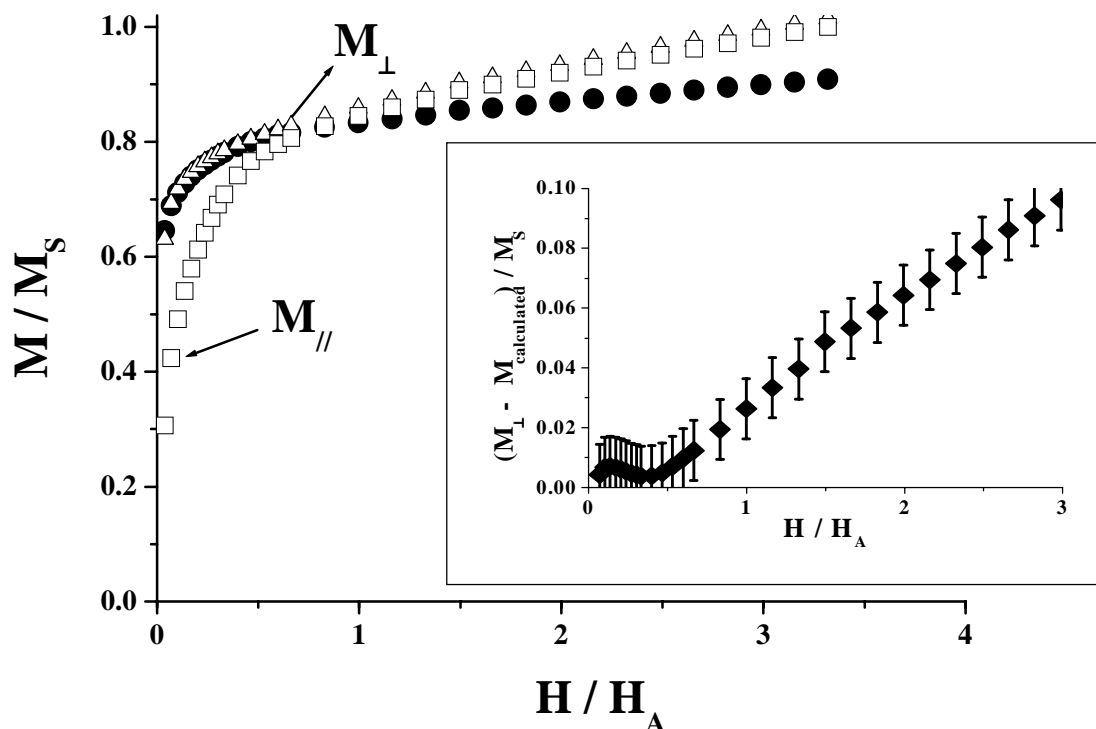


Fig. 1: Magnetization curves measured at $T=300\text{K}$ along the EMD, M_{\perp} (open triangles), the hard direction, M_{\parallel} (open squares) and the calculated EMD curve (circles) using the texture parameters versus H/H_A (with $H_A = 3\text{T}$, for details see the text). In the insert is represented the difference between M_{\perp} observed curve and the calculated one.

The powder neutron diffraction experiments performed at room temperature show that the $\text{ErMn}_4\text{Fe}_8\text{C}$ compound is ferrimagnetic (antiparallel Er-3d coupling scheme) with a magnetic structure belonging to the \mathbf{ab} -planes of the tetragonal structure [11].

Quantitative texture analysis were performed on Sample B (oriented carbide with H_{text} perpendicular to the z -axis), sample having a configuration corresponding to the macroscopic

EMD. We firstly verified that no significant change in the diffracted lines occurred when rotating the sample around the azimuth φ axis of the diffractometer, aligned parallel to z . The average reliability factor obtained for the refinement of the ODF is of only 1.2 %. The $\{001\}$ and $\{100\}$ pole figures (Fig. 2, left) are representative of a fiber texture with $\{001\}$ planes preferentially aligned perpendicular to the cylinder z -axis (normal of the figure plane) with a maximum orientation density about 3.9 m.r.d., showing a relatively low texture strength. A second minor orientation is observed with the $\{001\}$ planes parallel to this axis. The minimum orientation density of 0.5 mrd indicates that 50% of the sample volume is randomly oriented. From the point of view of the magnetic anisotropy, it is important to check if $\{hkl\}$ planes align with their normals along z , as can be directly seen on the inverse pole figure calculated for the z direction (Fig. 2, right). We retrieve the $\{001\}$ major and the $\{100\}$ minor components, but also two other minor ones: $\{221\}$ and $\{201\}$. The texture index F^2 equal to 1.3 mrd² and the entropy S equal to -0.13 indicate a relatively weak texture [4] but this orientation (4 m.r.d.) would be sufficient to induce a large anisotropy of the magnetic behavior.

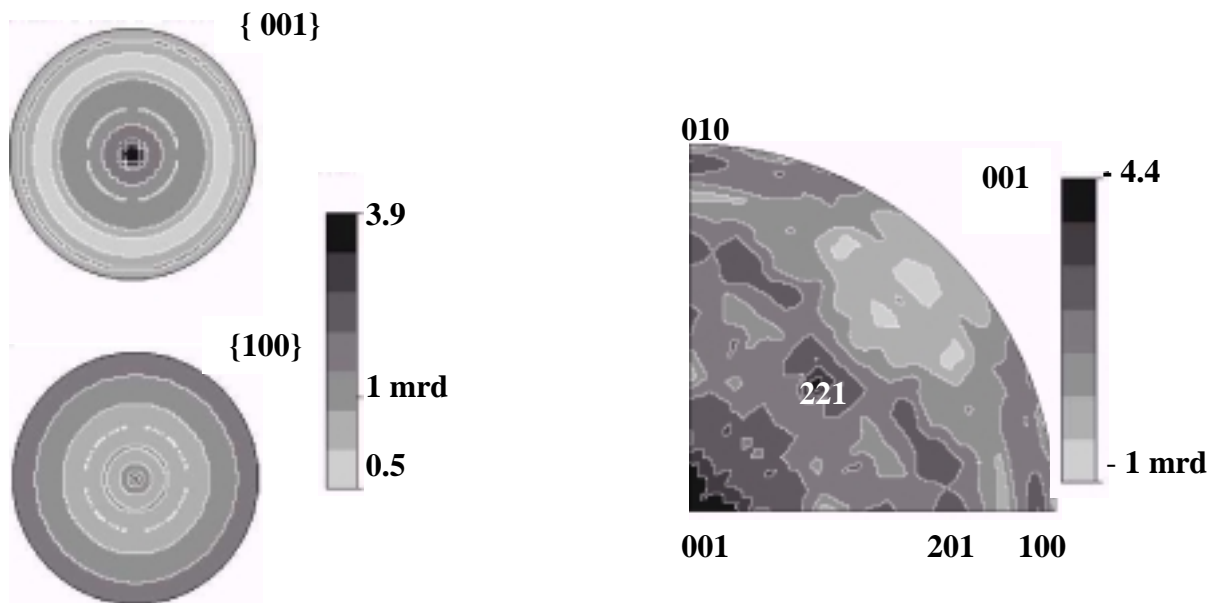


Fig. 2: Low-indices $\{001\}$ and $\{100\}$ recalculated pole figures from the ODF (right column) and (left column) inverse pole figure (001).

Considering that the z -direction is a c_∞ axis, we deduce that the function $F(\vartheta, \varphi)$ is composed of a radial distribution $G(\vartheta)$ and a constant $H(\varphi)$. The distribution $G(\vartheta)$ reflects the crystallite distribution function if the magnetic moments are linked to specific crystal axes, as revealed here by the neutron diffraction analysis. In our case, $G(\vartheta)$ corresponds to the radial pole profile $\{001\}$ recalculated from the ODF and corresponding to the c -axes distribution (Fig. 3). For such texture it comes that $\vartheta = \theta_0$ (Sample B) and the component of the magnetization along H , M_\perp , is [from Eq. (2) and incorporating the ODF]:

$$\frac{M_\perp}{M_s} = 2\pi \int_0^{\frac{\pi}{2}} G(\theta_0) \sin\theta_0 \cos(\theta_0 - \theta) d\theta_0 \quad (3)$$

where θ is calculated with the Eq. (2) for every value of H and θ_0 .

For a rotation aligned sample, $G(\vartheta)$ can be described by a Gaussian or a Lorentzian distribution of the z -axis [5,9]. We found a best fit for $G(\vartheta)$ (Fig. 3) having a Pseudo-Voigt shape, $PV(\vartheta)$, with a Half-Width at Half Maximum (HWHM) of 12.2° and a randomly distributed part of the volume, $\rho_0=0.5$ m.r.d. (minimum of distribution).

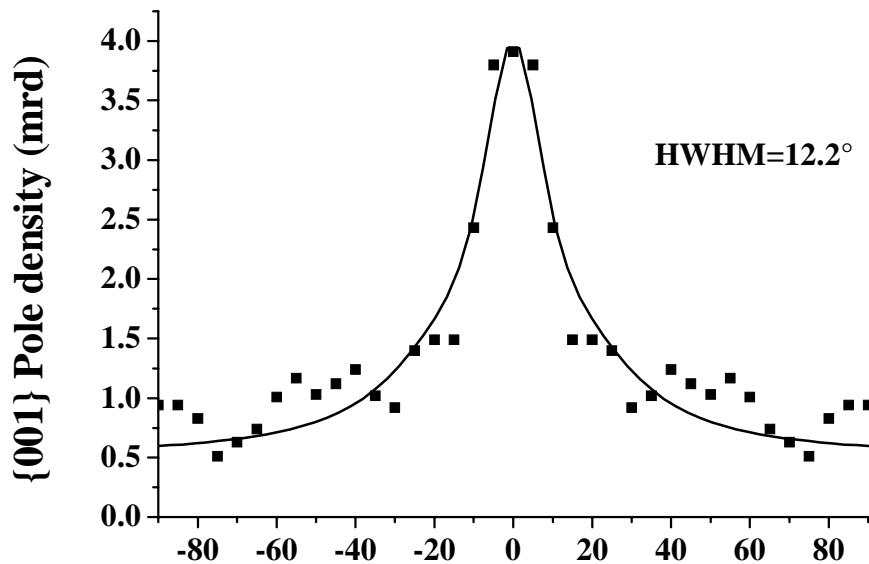


Fig. 3: Pseudo-Voigt fit of the {001} radial orientation distribution density of Sample B (M_{\perp}) deduced from the ODF refinement.

From the definition of the pole figures, ρ_0 is directly the random volume ratio, which contribution is the classical random magnetic signal M_r measured on the free powder weighted by its volume ratio in the measured textured sample. The contribution to the magnetization of the textured part is weighted by the remaining volume $(1-\rho_0)$ and Eq. (3) rewrites:

$$\frac{M_{\perp}}{M_s} = 2\pi \int_0^{\frac{\pi}{2}} (1-\rho_0) PV(\theta_0) \sin \theta_0 \cos(\theta_0 - \theta) d\theta_0 + \rho_0 \frac{M_r}{M_s} \quad (4)$$

with our determined values $M_s=6.37\mu_B/fu$, $H_A=3T$ and $\rho_0=0.5mrd$.

Using this model, we have simulated the experimental magnetization curves M_{\perp}/M_s of Sample B at $T=300K$ (Fig. 1). We observe a good agreement between these two curves for H/H_A values lower than 0.75 (insert of Fig.1). For higher magnetic fields ($H > 1.8 T$) the observed deviation may be attributed to pure magnetic effects, like for instance a First Order Magnetization Process (FOMP) [10], whereas a direct analysis of the magnetization curves would be unable to provide such a clear evidence. The FOMP results with the application of a magnetic field out of the easy-plane magnetization and reveals highly competing contributions between both the magneto-crystalline anisotropy terms and within the different exchange forces acting between the 3d and 4f sublattices.

To our knowledge, it is the first time that an experimental determination of texture is taken as input information for the magnetization curve calculation of an easy-plane ferrimagnetic compound. An important input of this approach is that the angular distribution

of the moments, the sample polarization and the crystalline anisotropic constant K_1 are taken into account in the simulation of the magnetization curves as measured parameters contrarily to previous work based on the studies of easy-axis ferromagnetic compounds [5,9]. Consequently, using this methodology, the texture effect of easy-plane ferrimagnetic carbide is clearly independently identified by X-ray analysis, and the observed difference between measured and simulated magnetization curves is associated to a pure magnetic effect. Furthermore, a later aspect of the QTA analysis should be mentioned. The way used to refine the ODF can introduce uncontrolled artifacts. Some authors [9, 16] used in order to fit magnetization curves the generalized harmonic formalism. This formalism implicitly necessitates that the texture can be represented by a specific function (spherical harmonics) using few textural parameters, with subsidiary ghost corrections, in order to remove negative distribution densities. There is no physically identified process in our texturation techniques that must imply specific distribution shapes that should be represented by specific functions, and we preferred to use a direct determination of the ODF with an intrinsic ghost correction.

The formalism developed in this work can *a priori* be extended to any other texture types, even presenting several texture components. For a better description of the FOMP, these texture measurements must be extended at low temperatures using both X-ray and neutron techniques, which will enable us to account higher anisotropy constants (normally negligible at room temperature), enhanced probably comparison to the parent RT₁₂ compounds [12, 17].

Acknowledgements

This work has been funded by the European Union project under the Growth program (G6RD-CT99-00169) ESQUI: "X-ray Expert System for Electronic Films Quality Improvement".

References

- [1] P. Weiss and R. Forrer: Ann. de Phys. Vol. 12 (1929), p. 279.
- [2] P. Gillon: Mat. Sci. and Eng. Vol. A287 (2000), p. 147.
- [3] B. Legrand et al.: J. Alloys and Comp. Vol. 275-277 (1998), p. 660.
- [4] S. Rivoirard et al.: Phil. Mag. Vol. A80 (2000), p. 1955.
- [5] W. Qun et al.: J. of Mag. and Magn. Mat. Vol. 109 (1992), p. 59.
- [6] C. W. Searle, V. Davis and R.D. Hutchens: J. Appl. Phys. Vol. 53 (1982), p. 2395.
- [7] K. Elk and R. Hermann: J. Mag. and Mag. Mat. 138, 138 (1993).
- [8] A. Yan, W. Zhang, H. Zhang and B. Shen: J. Mag. and Mag. Mat. Vol. 210 (2000), L10.
- [9] T. Walker et al.: Mikrochim. Acta 125, 355 (1997).
- [10] H. S. Li and J. M. D. Coey : *Handbook of Magnetic Materials* (K. H. J. Buschow, North Holland, Amsterdam, 1991) Vol. 6, p.1-83.
- [11] M. Morales et al.: J. Mag. and Mag. Mat. Vol. 236 (2001), p. 83.
- [12] H. Fujii and H. Sun : *Handbook of Magnetic Materials* (K. H. J. Buschow, North Holland, Amsterdam, 1991) Vol. 9, p. 356-363.
- [13] R. Vert et al.: J. Alloys and Comp. Vol. 287 (1999), p. 38.
- [14] J. Ricote, D. Chateigner: *Boletín de la Sociedad Española de Cerámica y Vidrio*, Vol. 38 (1999), p. 587-591.
- [15] S. Matthies and G.W. Vinel: Phys. Stat. Sol. vol. B112 (1982), K111.
- [16] M. Birsan, J. A. Szpunar: J. of Appl. Phys. Vol. 79(8) (1996), p. 5202-5204.
- [17] D. P. F. Hurley and J. M. D. Coey: J. Phys. Condens. Matter Vol. 4 (1992), p. 5573.